

Exotic Superfluid with Emergent Flux in a One-Dimensional Bose-Fermi Mixture

Qi Song,¹ Jie Lou,^{1,*} and Yan Chen^{1,2,†}

¹*Department of Physics and State Key Laboratory of Surface Physics, Fudan University, Shanghai 200433, China*

²*Shanghai Branch, Hefei National Laboratory, Shanghai 201315, P.R. China*

(Dated: May 9, 2024)

We find a novel chiral superfluid (CSF) phase in a chain of Bose-Fermi mixture, which has been validated using two unbiased numerical methods, density matrix renormalization group and Grassmann multi-scale entanglement renormalization ansatz. The system hosts the interplay between two types of fermions: bare spinless fermions and composite fermions, the latter consisting of a fermion and a boson. In the CSF phase, bosons condensate at non-zero momentum $\pm 2\pi/L$ with chain length L . The local superfluid order parameter continuously rotates along the chain, indicating that the CSF phase spontaneously breaks time-reversal symmetry. This symmetry breaking gives rise to an emergent flux in the background, effectively optimizing the kinetic energy of the composite fermions within the system. We provide a physical understanding at the mean-field level. Furthermore, we demonstrate that the 1D CSF phase can emerge in a more widely applicable extended Hubbard model. The potential realization of this phase in cold-atom experiments has also been explored.

The quest for unconventional novel superfluids[1–8] has been a persistent research focus in quantum physics. In fermionic systems, significant theoretical and experimental efforts spanning decades have been dedicated to topological superfluids[9, 10] and the Fulde-Ferrell-Larkin-Ovchinnikov state with finite-momentum Cooper pairs[11]. In bosonic systems, superfluid phases exhibiting complex order parameters have been experimentally observed in two-dimensional optical lattices[2–4], and the Potts-nematic superfluidity, which exhibits spontaneous rotation symmetry breaking, has also been reported[5]. Since Bose-Fermi mixtures (BFMs) incorporate both bosonic and fermionic degrees of freedom, the pursuit of novel superfluids within these mixtures presents a promising prospect.

The interaction between bosons and fermions is essential in condensed matter physics and can give rise to exotic states of matter. In conventional superconductors, phonon exchange between electrons triggers the formation of Cooper pairs[12]. Over the last two decades, ultracold bosonic and fermionic atoms have emerged as remarkable platforms for simulating quantum physics[13–15]. Due to their high controllability, atomic mixtures have exhibited rich phenomena, such as double superfluids[16–18], mediated interactions[19], heteronuclear molecules[20–22], and hybridized sound modes[23, 24]. Furthermore, topological p -wave superfluids in BFMs have garnered theoretical attention[25, 26]. Remarkably, spontaneous translational symmetry-breaking insulating states have recently been observed in two distinct solid-state BFM systems[27–29]. Consequently, BFMs are fertile ground for cultivating intriguing new superfluid phases.

In this paper, we reveal a novel chiral superfluid (CSF) phase that spontaneously breaks time-reversal symmetry. In this phase, the bosonic superfluid order rotates along the chain, resulting in an effective emergent flux. The system we investigate exhibits a complex interplay

between bare spinless fermions and composite fermions (consisting of a fermion and a boson) in a 1D BFM. In the presence of composite hopping, where a fermion hops with a boson, the tunneling processes of fermions and bosons become correlated. Remarkably, the system solely adopts the CSF as its ground state when an even number of fermions are present in the mixture. Conversely, it transitions to a conventional superfluid state when the number of fermions is odd. This indicates that the chirality of this quantum system, protected by an energy gap, can be manipulated by adding or removing particles through the tuning of chemical potentials. This even-odd disparity underscores the topological nature of the CSF. The CSF phase can be directly realized within the conventional extended Bose-Fermi Hubbard model. We provide numerical evidence and discuss the possibility of realizing the 1D CSF in cold-atom experiments.

Emergence of CSF phase.— We introduce a minimal model that incorporates the motion of composite fermions (CFs) $-t_{cf}c_i^\dagger b_i^\dagger c_j b_j$, which describes the binding and hopping of a fermion and a boson. The resulting Hamiltonian for our system reads

$$H = -t_f \sum_{\langle ij \rangle} (c_i^\dagger c_j + H.c.) - t_{cf} \sum_{\langle ij \rangle} (c_i^\dagger b_i^\dagger c_j b_j + H.c.) + \frac{U_{bb}}{2} \sum_i n_i^b (n_i^b - 1) - \mu_b \sum_i n_i^b - \mu_f \sum_i n_i^f \quad (1)$$

where U_{bb} represents the onsite repulsive interaction between bosons, $n_i^b (n_i^f)$ is the onsite boson (fermion) number operator, and $\mu_b (\mu_f)$ is the chemical potential of bosons (fermions). We consider the case $N_f > N_b$.

We employ both the density matrix renormalization group (DMRG)[31, 32] and Grassmann multi-scale entanglement renormalization ansatz (GMERA)[33] methods, two well-established unbiased numerical techniques based on tensor product ansatz to study this BFM model.[34] Our calculations reveal an intriguing outcome: due to

strong scattering interactions, bosons decouple from composite particles and enter a superfluid state when $t_{cf} < t_f$. More remarkably, when the number of fermions N_f in the system is even, the bosons condense at non-zero momentum $k_0 = \pm 2\pi/L$, where L represents the size of the periodic chain (Fig. 3). In contrast to conventional superfluids, where condensation occurs at $k = 0$, this non-zero momentum condensation leads to a complex local order parameter $\langle b_i \rangle$ that rotates continuously along the chain. The twisted angles θ_{ij} (argument difference between $\langle b_i \rangle$ and $\langle b_j \rangle$ on two neighboring sites (i, j)) add up to 2π over a complete lattice period, as illustrated in Fig. 1. This chiral superfluid (CSF) state spontaneously breaks time-reversal symmetry, resulting in a unique and intriguing emergent flux state in the Bose-Fermi mixture.

We address the origin of CSF from two distinct perspectives, starting from the bare fermion limit ($t_f \gg t_{cf}$). First, the kinetic term of composite particles (t_{cf}) suggests that a bosonic superfluid in the background induces projected "silhouette" composite particles. A CSF introduces an additional phase factor that fermions acquire during hopping. Effectively, this generates an "emergent flux" that further improves the system energy, analogous to the behavior of electrons hopping in a ring with a magnetic flux[35]. Based on this argument, we develop a mean-field consideration, resulting in an effective boson-free model that qualitatively aligns with our original Hamiltonian in the bare fermion limit. Second, the fermionic response to the bosonic emergent flux is crucial. As the CSF emerges, it profoundly modifies the fermionic momentum distribution. Numerical calculations reveal that the degeneracy of the fermionic Fermi surface (two Fermi points) is lifted simultaneously when the time-reversal symmetry of the superfluid is broken. This lifting of degeneracy is accompanied by a redistribution of the momentum distribution of composite particles, which becomes more concentrated around small k values, further optimizing the system's energy. The collaborative effect between the fermionic and bosonic sectors stabilizes the CSF state.

CSF and Fermions parity.— Furthermore, our system exhibits an intriguing sensitivity to the parity of fermions. Specifically, when the number of fermions N_f is even, the ground state is in the CSF phase where bosons condensation occurs at $k_0 = \pm 2\pi/L$, either clockwise or counterclockwise, depending on the sign of k_0 . However, when N_f is odd, bosons condense at $k = 0$, similar to a conventional superfluid. In both cases, the superfluid phase persists to an intense competition region $t_f \approx t_{cf}$. Numerical results from the long-range boson correlation $G_b(x) = \langle b_i^\dagger b_{i+x} \rangle$ and momentum distribution $n_b(k)$ show that superfluidity emerges as soon as t_{cf} is turned on, such as ($t_{cf} = 10^{-3}t_f$). In the weakly coupled case, with a boson superfluid as the background, we understand that the free hopping fermions can gain additional energy through the t_{cf} term in Eqn. 1, by projecting

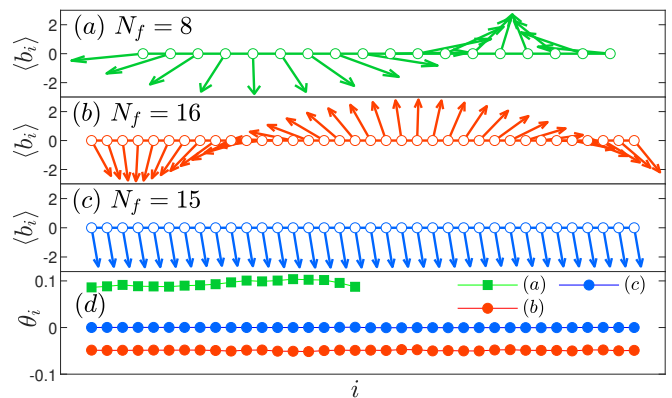


FIG. 1. (a)–(c): The boson superfluid order parameter $\langle b_i \rangle$ (arrows) measured on each site i (open circles), magnified ten times, with the horizontal/vertical component of the arrow corresponding to its real/imaginary part, respectively. (d): The argument angle θ_i of the nearest-neighbor hopping term $\langle b_i^\dagger b_{i+1} \rangle$. Results are obtained at parameter setting $t_f = 0.2, t_{cf} = 0.4, U_{bb} = 3.0$.

out silhouette composite particles. When N_f is even, the energy contribution from the t_{cf} term can be further optimized by allowing superfluid order parameter $\langle b \rangle$ to rotate and acquire chirality. In such cases, the hopping amplitude $\langle b_i^\dagger b_j \rangle$ becomes a complex number due to the phase difference of $\langle b \rangle$ between neighboring sites. Consequently, the expression $c_i^\dagger c_j b_i^\dagger b_j$ should be regarded as $c_i^\dagger c_j \langle b_i^\dagger b_j \rangle$. Numerical results confirm that the measurement of $\langle b_i^\dagger b_j \rangle$ on different bond $\langle i, j \rangle$ exhibit nearly identical arguments and moduli, as shown in Fig. 1(d). This observation suggests that a CSF generates an additional phase factor $e^{i\theta_{ij}}$ in the composite hopping term.

Explanation from effective flux.— The above finding enlightens us to trace back to the "flux phase" problem [36–39] which provides insight into why magnetic flux can lower the ground-state energy of fermions. Extensive studies have shown that the energy of electrons can be improved by the presence of magnetic flux penetrating the lattice, both in one-dimensional (1D) systems [40] and in higher dimensions [41–43]. In the specific case of spinless fermions in 1D, rigorous theoretical works [44–46] have established that the optimal total flux phase $\Phi = \pi$ when N_f is even, 0 otherwise.

Next we apply a mean-field approximation to our Hamiltonian (1) to acquire a corresponding boson-free model

$$H_{MF} = -t_f \sum_{\langle ij \rangle} (c_i^\dagger c_j + H.c.) - t'_{cf} \sum_{\langle ij \rangle} (c_i^\dagger c_j e^{i\theta_{ij}} + H.c.)$$

The second term can be intuitively understood through our mean-field ansatz, treating the influence of bosons classically as a pure phase factor $e^{i\theta_{ij}}$. Therefore, we substitute the hopping term $c_i^\dagger b_i c_{i+1} b_{i+1}^\dagger$ with $c_i^\dagger c_j e^{-i\theta}$. This model highlights the two competing hopping processes:

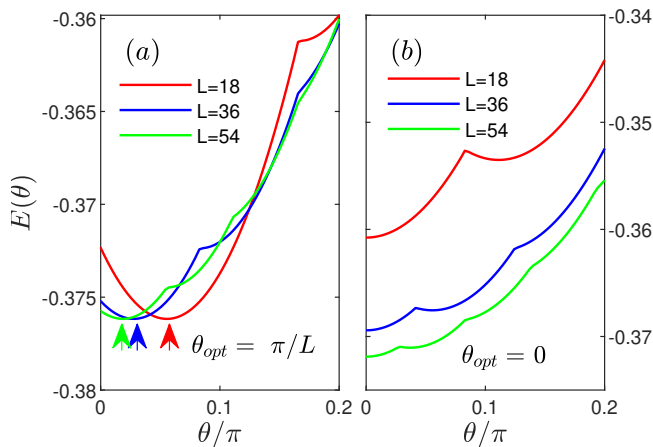


FIG. 2. The ground state energy $E(\theta)$ of the mean-field Hamiltonian H_{MF} as a function of the argument θ in $L = 18, 36, 54$ systems when $t_f = 0.2, t_{cf} = 0.4$. (a) Even fermion parity. The fermion filling factor is fixed at $n_f = N_f/L = 4/9$. There is a prominent peak on $\theta = 0$ where no magnetic flux is threaded through the system. And $E(\theta)$ reaches its absolute minimum at $\theta_{opt} = \pi/L$. (b) Odd fermion parity. N_f are 7, 15, 23 for $L = 18, 36, 54$ respectively. No peak shows on $\theta = 0$ contrary to the even case in the main panel. And $E(\theta)$ reaches its absolute minimum at $\theta_{opt} = 0$

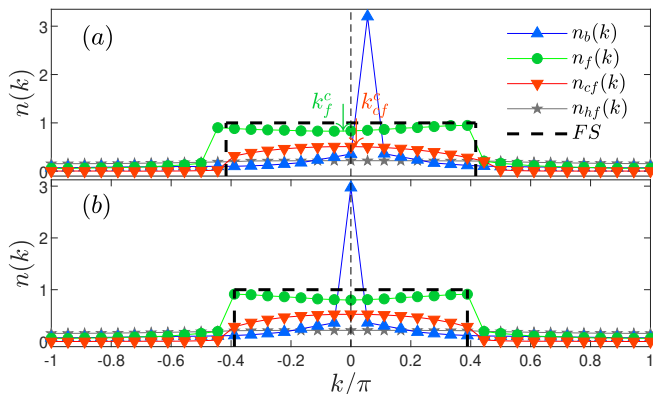


FIG. 3. Momentum distribution functions $n(k)$ for $L = 36$ system with boson filling factor $n_b \approx 1/4$, obtained by GMERA. "FS" refers to the symmetric Fermi surface of original fermions. (a) For $N_f = 16$ (even), bosons condensate at $|k_0| = 2\pi/L$ (position of the blue peak in $n_b(k)$). $k_f^c = \sum_k n_f(k) \times k/N_f = -0.0122\pi$ is the center of original Fermi sea, whereas $k_{cf}^c = \sum_k n_{cf}(k) \times k/N_{cf} = 0.0075\pi$ is the center of Fermi sea for composite fermion, where $N_{cf} = \sum_k n_{cf}(k)$. (b) For $N_f = 15$ (odd), bosons condensate at $k = 0$. The parameters are chosen as $t_f = 0.2, t_{cf} = 0.4, U_{bb} = 3.0$. Fourier transforms of $G_b(i, j) = \langle b_i^\dagger b_j \rangle$, $G_f(i, j) = \langle c_i^\dagger c_j \rangle$, $G_{cf}(i, j) = \langle c_i^\dagger b_i^\dagger c_j b_j \rangle$ and $G_{hf}(i, j) = \langle c_i^\dagger b_i c_j b_j^\dagger \rangle$ give respective momentum distributions $n_b(k)$, $n_f(k)$, $n_{cf}(k)$ and $n_{hf}(k)$. The black dashed lines guide the eyes at $k = 0$.

the former stands for original free hopping, whereas the latter depicts hoppings experiencing a lattice flux. This simple model can be solved straightforwardly. As shown in Fig. 2, the ground state energy E exhibits a periodically varying function superimposed on a parabolic background, illustrating the competition between two distinct hopping processes. Remarkably, a significant difference is also observed between systems with even (left panel) and odd (right panel) fermion parity: when N_f is even, the optimal θ equals to π/L . In contrast, when N_f is odd, the optimal θ takes the value of 0. This observation from the mean-field model is similar to the results obtained in the BFM. However, it is crucial to note that θ_{ij} , the argument of the complex $\langle b_i^\dagger b_{i+1} \rangle$ shown in Fig. 1(d), averages out to 0.0940π for $L = 18$ or -0.0491π for $L = 36$, deviating from the optimal angle of $\pm\pi/L$ predicted by mean-field theory. This deviation is attributed to the periodic boundary conditions imposed on our homogeneous lattice.

Shift of Fermi surface.— Interplay and correlations between different species of particles lead to the shift of the Fermi surface. We focus on the correlation function and momentum distribution of involved particles, influenced by the effective flux. When N_f is odd, the conventional bosonic superfluid serves as a flux-free background, the correlation function of projected composite fermion $G_{cf}(i, j) = \langle c_i^\dagger b_i^\dagger c_j b_j \rangle$ shows similar long-range behavior as that of an original fermion. As demonstrated in Fig. 3, two clear Fermi surfaces (points) of composite particles have the same momentum as those of spinless fermions. In contrast, when N_f is even, the ground state exhibits a two-fold degeneracy: bosons condensate at either $+2\pi/L$ or $-2\pi/L$, time-reversal symmetry of the system is spontaneously broken. Intriguingly, this degeneracy lift simultaneously affects the Fermi surface of a bare fermion. The selection of the last filled momentum is determined by the direction of the effective flux, resulting in an asymmetric bulk of the Fermi surface. Consequently, the Fermi surface of the projected composite fermion shifts towards $k = 0$, optimizing the system's overall energy. In this uncorrelated limit, this projection can be rationalized as follows: $n_{cf}(k) = 1/L \sum_{i,j} G_{cf}(i, j) e^{ik(x_i - x_j)} \approx 1/L \sum_{i,j} G_f(i, j) G_b(i, j) e^{ik(x_i - x_j)} \approx 1/L \sum_{i,j} G_f(i, j) |A| e^{i(k+k_0)(x_i - x_j)}$. Here, $G_b(i, j) = |A| e^{ik_0(x_i - x_j)}$ represents the boson correlation for superfluid condensates at momentum k_0 .

By carefully comparing DMRG and GMERA results, we confirm that the CSF phase is energetically favorable. DMRG calculations often maintain degeneracy and symmetry, as evident in Fig. 5. Conversely, GMERA outcomes are prone to symmetry-breaking. In Fig. 3, we present the momentum distribution derived from GMERA calculations. Please refer to the Supplementary Material [34] for further details.

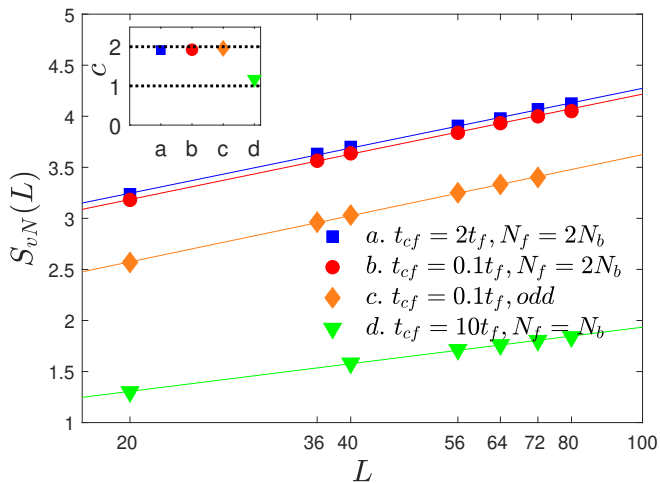


FIG. 4. The entanglement entropy S_{vN} as a function of L at different values of t_{cf}/t_f and fermion parity. Boson and fermion numbers are $N_f = N_b = L/2$ in 'a' (blue solid squares) and 'b' (red solid circles), $N_f = L/2 - 1$, $N_b = L/2$ in 'c' (orange solid diamonds) and $N_f = N_b = L/2$ in 'd' (green solid triangles). Inset shows the results of central charge.

Comments about strong correlations.— Although the previous explanation is based on the uncorrelated limit, the CSF phase remains remarkably stable up to $t_f \approx t_{cf}$. A noteworthy difference emerges between $\langle c_i^\dagger b_i^\dagger c_{i+1} b_{i+1} \rangle$ and $\langle c_i^\dagger b_i c_{i+1} b_{i+1}^\dagger \rangle$ that grows as t_{cf} increases. This distinction suggests a deviation from the uncorrelated scenario since a straightforward uncorrelated superfluid background fails to distinguish between these two terms. Additional evidence can be found in the momentum distribution $n(k)$ of the intermediate region. The singularity of the Fermi surface for spinless fermions and composite particles is significantly altered by strong correlations, manifesting as convex and concave features in $n(k)$ near $k = 0$ due to strong scattering.

Intriguingly, the central charge obtained from entanglement entropy in DMRG calculations remains consistently ≈ 2 , as illustrated in Fig. 4. This observation indicates that, despite the projected particle's contribution to optimizing the system's total energy, it resembles the original particles. Global excitations are contributed by bosons superfluid and fermions Luttinger liquid. It is worth mentioning that the condensation of a bosonic superfluid at a momentum $k \neq 0$ has been previously explored in various works, including those studying systems with correlated hopping [47, 48], as well as in the experimental realization of a two-dimensional topological chiral superfluid observed in optical lattice experiments [2–4]. Nevertheless, the microscopic origin of the one-dimensional CSF in our system is fundamentally different. It arises directly from the interplay between two species of fermions and serves as a background field to optimize the system's overall energy.

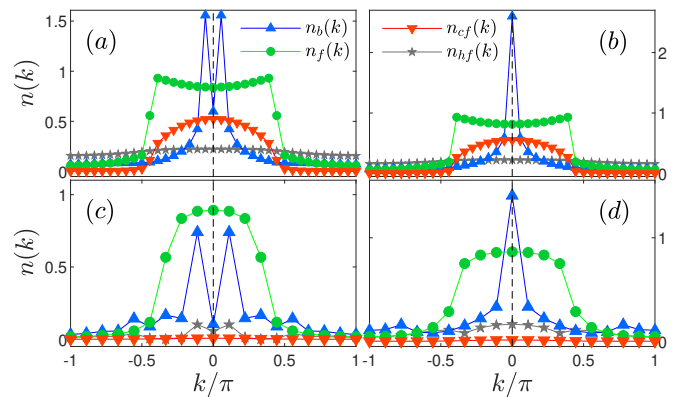


FIG. 5. Momentum distribution functions $n(k)$ obtained by DMRG. (a) $N_f = 16 = 2N_b$ and (b) $N_f = 15$, $N_b = 8$ correspond to the Hamiltonian (1) at $t_{cf} = 2t_f$ and $t_{cf} = 0.4$ for $L = 36$ sites. (c) $N_f = 6$, $N_b = 3$ and (d) $N_f = 7$, $N_b = 4$ correspond to the extended BF Hamiltonian (2) at $t_f = 0.4$, $t_b = 0.05$, $U_{bb} = 3.0$, $U_{bf} = 3.0$, $V_{bf} = -0.3$ for $L = 18$ sites. For even N_f (Left column), bosons condensate at $|k_0| = 2\pi/L$ (positions of the two blue peaks in $n_b(k)$). For odd N_f (right column), bosons condensate at $k = 0$.

CSF in Extended BF Hubbard Model.— We have elucidated the origin of the 1D CSF phase using a model that incorporates the kinetic energy of composite fermions. However, this seemingly “artificial” term is not an indispensable component. The 1D CSF phase may naturally arise in the extended BF Hubbard model, which is given by

$$H_{BF} = - \sum_{\langle ij \rangle} (t_f c_i^\dagger c_j + t_b b_i^\dagger b_j + H.c.) + U_{bf} \sum_i n_i^b n_i^f + \frac{U_{bb}}{2} \sum_i n_i^b (n_i^b - 1) + \frac{V_{bf}}{2} \sum_{\langle ij \rangle} (n_i^b n_j^f + n_i^f n_j^b). \quad (2)$$

where t_b represents the hopping amplitude of bosons, while $t_f, U_{bb}, n_i^b, n_i^f$ retain the same meanings as in Hamiltonian (1).

Here we introduce an asymmetry by setting an unequal number of bosons and fermions. This asymmetry leads to strong scattering of composite particles by surplus fermions, resulting in instability. The Hamiltonian incorporates a standard on-site boson-fermion repulsion term U_{bf} [49], facilitating the formation of composite particles. To prevent phase separation, a nearest-neighbor attraction V_{bf} is introduced. The filling factor of fermion is less than $1/3$ to avoid collapse state[50] and $N_f \approx 2N_b$. When $t_f \approx 10t_b$ and U_{bf} is one order larger than t_f ($U_{bf} = U_{bb}$), DMRG simulations show that bosons condensate at $|k_0| = 2\pi/L$ with even fermion number N_f , as shown in Fig. 5(c) similar to that in Fig. 5(a). For odd N_f in Fig. 5(d), bosons condensate at $k = 0$ similar to that in Fig. 5(b). The fermions parity-dependent chirality provides further confirmation, which suggests that this novel chirality can be controlled by simply adding or

removing particles through tuning chemical potentials. The realization of the CSF phase is more feasible in practical experimental settings.

Experimental feasibility.— With the thriving development of quantum simulation experiments[13–15, 51], our model is promising to be effectively simulated in an optical lattice utilizing a combination of ultracold bosonic and fermionic atoms[20, 21, 52, 53]. Experimentally, periodic boundary conditions have been achieved in a 1D ring-shaped optical lattice with finite sites[54–58]. The characteristic signature of the CSF phase can be observed through widely utilized time-of-flight (TOF) experiments, which restore phase coherence information throughout the entire lattice[13, 59]. The density distribution captured in TOF images corresponds to the momentum distribution of the trapped atoms. During TOF expansion, the fermionic atoms influenced by an effective flux induced by the bosonic CSF will exhibit a doughnut-shaped pattern (analogous to the right panel of Fig.5 in Ref.[58]). This pattern contrasts with the bell-shaped pattern observed when bosons are in a normal superfluid state and fermions experience no effective flux [58].

Conclusions.— Our study reveals a novel many-body effect in a 1D BFM system, where the CSF phase emerges as the ground state and spontaneously breaks TSR to optimize the energy of the whole system. Concrete numerical evidence and theoretical analysis provide a comprehensive understanding of the origin of CSF. Notably, the ground state can be tuned between the CSF and a conventional superfluid by adjusting chemical potentials. Furthermore, we demonstrate the experimental feasibility of realizing this innovative state. Our discovery opens up opportunities to explore new quantum phases of matter.

We thank Ting-Kuo Lee and Kai Chang for their fruitful suggestions. This work is supported by the National Key Research and Development Program of China Grant No. 2022YFA1404204, and the National Natural Science Foundation of China Grant No. 12274086.

* loujie@fudan.edu.cn

† yanchen99@fudan.edu.cn

- [1] W. Chen, C.-J. Huang, and Q. Zhu, *Phys. Rev. Lett.* **131**, 236004 (2023).
- [2] X.-Q. Wang, G.-Q. Luo, J.-Y. Liu, W. V. Liu, A. Hemmerich, and Z.-F. Xu, *Nature* **596**, 227 (2021).
- [3] T. Kock, M. Ölschläger, A. Ewerbeck, W.-M. Huang, L. Mathey, and A. Hemmerich, *Phys. Rev. Lett.* **114**, 115301 (2015).
- [4] P. Soltan-Panahi, D.-S. Lühmann, J. Struck, P. Windpassinger, and K. Sengstock, *Nature Physics* **8**, 71 (2012).
- [5] S. Jin, W. Zhang, X. Guo, X. Chen, X. Zhou, and X. Li, *Phys. Rev. Lett.* **126**, 035301 (2021).
- [6] X. Li, Z. Zhang, and W. V. Liu, *Phys. Rev. Lett.* **108**, 175302 (2012).
- [7] D.-S. Lühmann, *Phys. Rev. A* **94**, 011603(R) (2016).
- [8] Z.-F. Xu, L. You, A. Hemmerich, and W. V. Liu, *Phys. Rev. Lett.* **117**, 085301 (2016).
- [9] J. C. Wheatley, *Rev. Mod. Phys.* **47**, 415 (1975).
- [10] M. Sato and Y. Ando, *Reports on Progress in Physics* **80**, 076501 (2017).
- [11] J. J. Kinnunen, J. E. Baarsma, J.-P. Martikainen, and P. Törmä, *Reports on Progress in Physics* **81**, 046401 (2018).
- [12] J. Schrieffer, *Theory of Superconductivity*, Advanced Book Program Series (Avalon Publishing, New York, 1983).
- [13] I. Bloch, J. Dalibard, and W. Zwerger, *Rev. Mod. Phys.* **80**, 885 (2008).
- [14] C. Gross and I. Bloch, *Science* **357**, 995 (2017).
- [15] F. Schfer, T. Fukuhara, S. Sugawa, Y. Takasu, and Y. Takahashi, *Nature Reviews Physics* **2**, 411 (2020).
- [16] I. Ferrier-Barbut, M. Delehaye, S. Laurent, A. T. Grier, M. Pierce, B. S. Rem, F. Chevy, and C. Salomon, *Science* **345**, 1035 (2014).
- [17] R. Roy, A. Green, R. Bowler, and S. Gupta, *Phys. Rev. Lett.* **118**, 055301 (2017).
- [18] X.-C. Yao, H.-Z. Chen, Y.-P. Wu, X.-P. Liu, X.-Q. Wang, X. Jiang, Y. Deng, Y.-A. Chen, and J.-W. Pan, *Phys. Rev. Lett.* **117**, 145301 (2016).
- [19] B. J. DeSalvo, K. Patel, G. Cai, and C. Chin, *Nature* **568**, 61 (2019).
- [20] S. Inouye, J. Goldwin, M. L. Olsen, C. Ticknor, J. L. Bohn, and D. S. Jin, *Phys. Rev. Lett.* **93**, 183201 (2004).
- [21] C. A. Stan, M. W. Zwierlein, C. H. Schunck, S. M. F. Raupach, and W. Ketterle, *Phys. Rev. Lett.* **93**, 143001 (2004).
- [22] J. v. Milczewski and M. Duda, *Nature Physics* **19**, 624 (2023).
- [23] K. Patel, G. Cai, H. Ando, and C. Chin, *Phys. Rev. Lett.* **131**, 083003 (2023).
- [24] X. Shen, N. Davidson, G. M. Bruun, M. Sun, and Z. Wu, *Phys. Rev. Lett.* **132**, 033401 (2024).
- [25] Z. Wu and G. M. Bruun, *Phys. Rev. Lett.* **117**, 245302 (2016).
- [26] J. J. Kinnunen, Z. Wu, and G. M. Bruun, *Phys. Rev. Lett.* **121**, 253402 (2018).
- [27] D. A. Ruiz-Tijerina, *Nature Materials* **22**, 153 (2023).
- [28] Y. Zeng, Z. Xia, R. Dery, K. Watanabe, T. Taniguchi, J. Shan, and K. F. Mak, *Nature Materials* **22**, 175 (2023).
- [29] C. Lagoin, S. Suffit, K. Baldwin, L. Pfeiffer, and F. Dubin, *Nature Materials* **22**, 170 (2023).
- [30] K. Sheshadri and A. Chainani, *Phys. Rev. Res.* **2**, 023291 (2020).
- [31] S. R. White, *Phys. Rev. Lett.* **69**, 2863 (1992).
- [32] ITENSOR, <http://itensor.org>.
- [33] J. Lou and Y. Chen, (2015), [arXiv:1506.03716](https://arxiv.org/abs/1506.03716).
- [34] See supplementary materials.
- [35] D. Peter, M. Cyrot, D. Mayou, and S. N. Khanna, *Phys. Rev. B* **40**, 9382 (1989).
- [36] P. Wiegmann, *Physica C: Superconductivity* **153-155**, 103 (1988).
- [37] E. H. Lieb, *Helvetica Physica Acta* **65**, 247 (1992).
- [38] E. Lieb and M. Loss, *Duke Mathematical Journal* **71**, 337 (1993).
- [39] N. Macris and B. Nachtergaele, *Journal of Statistical Physics* **85**, 745 (1996).

- [40] F. Nakano, *Journal of Physics A: Mathematical and General* **33**, 5429 (2000).
- [41] Y. Hasegawa, P. Lederer, T. M. Rice, and P. B. Wiegmann, *Phys. Rev. Lett.* **63**, 907 (1989).
- [42] Y. Hasegawa, Y. Hatsugai, M. Kohmoto, and G. Montambaux, *Phys. Rev. B* **41**, 9174 (1990).
- [43] E. H. Lieb, *Phys. Rev. Lett.* **73**, 2158 (1994).
- [44] W. Nie, H. Katsura, and M. Oshikawa, *Phys. Rev. Lett.* **111**, 100402 (2013).
- [45] W. Nie, H. Katsura, and M. Oshikawa, *Phys. Rev. B* **97**, 125153 (2018).
- [46] W. Zheng, *Journal of Statistical Mechanics: Theory and Experiment* **2020**, 073103 (2020).
- [47] J. Struck, C. Ölschläger, M. Weinberg, P. Hauke, J. Simonet, A. Eckardt, M. Lewenstein, K. Sengstock, and P. Windpassinger, *Phys. Rev. Lett.* **108**, 225304 (2012).
- [48] T. Keilmann, S. A. Lanzmich, I. McCulloch, and M. Roncaglia, *Nature communications* **2**, 361 (2010).
- [49] L. Pollet, M. Troyer, K. Van Houcke, and S. M. A. Rombouts, *Phys. Rev. Lett.* **96**, 190402 (2006).
- [50] M. Rizzi and A. Imambekov, *Phys. Rev. A* **77**, 023621 (2008).
- [51] C. Weitenberg and J. Simonet, *Nature Physics* **17**, 1342 (2021).
- [52] A. G. Truscott, K. E. Strecker, W. I. McAlexander, G. B. Partridge, and R. G. Hulet, *Science* **291**, 2570 (2001).
- [53] T. Fukuhara, S. Sugawa, Y. Takasu, and Y. Takahashi, *Phys. Rev. A* **79**, 021601(R) (2009).
- [54] S. Franke-Arnold, J. Leach, M. J. Padgett, V. E. Lembessis, D. Ellinas, A. J. Wright, J. M. Girkin, P. Öhberg, and A. S. Arnold, *Optics Express* **15**, 8619 (2007).
- [55] L. Amico, A. Osterloh, and F. Cataliotti, *Phys. Rev. Lett.* **95**, 063201 (2005).
- [56] N. Houston, E. Riis, and A. S. Arnold, *Journal of Physics B: Atomic, Molecular and Optical Physics* **41**, 211001 (2008).
- [57] L. Amico, D. Aghamalyan, F. Auksztol, H. Crepaz, R. Dumke, and L. C. Kwek, *Scientific Reports* **4**, 4298 (2014).
- [58] L. Amico, D. Anderson, M. Boshier, J.-P. Brantut, L.-C. Kwek, A. Minguzzi, and W. von Klitzing, *Rev. Mod. Phys.* **94**, 041001 (2022).
- [59] M. Greiner, O. Mandel, T. Esslinger, T. W. Hnsch, and I. Bloch, *Nature* **415**, 39 (2002).